

The \tilde{X}^2B_1 , \tilde{A}^2B_2 , \tilde{B}^2A_1 , and \tilde{C}^2A_2 States of Cl_2O^+ : ab Initio Calculations and Simulations of the He I Photoelectron Spectrum

De-chao Wang,[†] Edmond P. F. Lee,[†] Foo-tim Chau,^{*,†} Daniel K. W. Mok,[†] and John M. Dyke[‡]

Department of Applied Biology and Chemical Technology, Hong Kong Polytechnic University, Hung Hom, Hong Kong, and Department of Chemistry, University of Southampton, Highfield, Southampton SO17 1BJ, UK

Received: November 5, 1999; In Final Form: January 26, 2000

CASSCF and QCISD calculations were carried out on the \tilde{X}^1A_1 state of Cl_2O and the \tilde{X}^2B_1 , \tilde{A}^2B_2 , \tilde{B}^2A_1 , and \tilde{C}^2A_2 states of Cl_2O^+ in order to obtain their minimum-energy geometries and harmonic vibrational frequencies. $Cl_2O^+ \leftarrow Cl_2O \tilde{X}^1A_1$ vertical and adiabatic ionization energies were also computed at the RCCSD(T)/QCISD level. Spectral simulations based on the ab initio results were performed for the first four bands of the He I photoelectron spectra of Cl_2O . Iterative Franck–Condon analyses were also carried out. Comparison between the simulated and the observed spectra gave, for the first time, experimentally derived geometries, for the \tilde{X}^2B_1 , \tilde{A}^2B_2 , and \tilde{C}^2A_2 cationic states. The adiabatic ionization energy position and the vibrational assignments of the $Cl_2O^+ \tilde{A}^2B_2 \leftarrow Cl_2O \tilde{X}^1A_1$ band were revised, based on spectral simulations, which included “hot” bands.

1. Introduction

The involvement of chlorine oxides in the loss of stratospheric ozone has motivated extensive studies into their photochemical, bonding, and spectroscopic properties.^{1,2} Dichlorine monoxide is thought to play only a minor role in the stratospheric ozone cycle. However, an understanding of the properties of this molecule can lead to an improved understanding of the more complex compounds of chlorine oxide, which play a more important role in the ozone cycle. Cl_2O is also frequently used as a source of ClO in laboratory studies and the synthesis of HOCl, a significant chlorine reservoir in the atmosphere. Furthermore, a correct interpretation of experiments, such as molecular beam studies to determine the yield of Cl and ClO fragments on photodissociation of Cl_2O , also requires characterization of Cl_2O photochemistry. Consequently, the photochemistry and near-ultraviolet (UV) spectroscopic properties of Cl_2O have received considerable attention in recent years from both experimentalists and theoreticians. Although the spectroscopy and photodissociation dynamics of Cl_2O have been extensively investigated using a wide range of techniques, there have been only a few studies on photoionization of Cl_2O .

The He I photoelectron (PE) spectrum of Cl_2O was first reported by Cornford et al. in 1971.³ With a spectral resolution of ca. 40 meV, only the lowest PE band of the spectrum was found to exhibit vibrational structure, which consisted of two progressions, assigned to excitation of the symmetric stretching vibrational mode, ν_1 , and the bending vibrational mode, ν_2 . The first adiabatic ionization energy (AIE) was measured to be 10.94 eV. Twenty-five years later, Thorn et al.⁴ deduced an AIE value of 10.909 ± 0.016 eV from the photoionization efficiency (PIE) spectrum of Cl_2O . Very recently, Motte-Tollet et al.⁵ reported a higher resolution He I PE study (with a full width at half-maximum, fwhm, of 20meV) of Cl_2O , in which four structured

bands were observed. New ionization energies were determined for the four lowest lying electronic states of the molecular ion. Additionally, microwave spectroscopy^{6,7} and electron diffraction experiments^{8,9} have shown that Cl_2O is bent in its electronic ground state, \tilde{X}^1A_1 , with its equilibrium bond length and bond angle being 1.6959 Å and 110.89°, respectively.

Cl_2O possesses a complex manifold of electronically excited states. The four highest occupied molecular orbitals are nearly degenerate nonbonding and weakly antibonding orbitals, and excitation of electrons from these orbitals gives rise to several transitions in the visible and ultraviolet regions.¹⁰ Nickolaisen et al.¹¹ reported CASSCF/MRCI calculations on neutral Cl_2O , which studied the energy ordering and oscillator strengths for singlet–singlet and triplet–triplet transitions. In addition, the G2 and G2 (MP2) energies of ClO, Cl_2O , ClO₂, and Cl_2O_2 have been reported by Luke.¹² However, to our knowledge, there has not been any ab initio study of the states of Cl_2O^+ or a simulation of the photoelectron spectrum of Cl_2O .

In the present study, we report ab initio calculations on the neutral ground state, and the \tilde{X}^2B_1 , \tilde{A}^2B_2 , \tilde{B}^2A_1 , and \tilde{C}^2A_2 states of Cl_2O^+ . From these calculations, the geometries and harmonic frequencies for the neutral and cationic states are obtained, as well as the adiabatic ionization energies (AIE) and vertical ionization energies (VIE) for the first four bands in the ultraviolet photoelectron spectrum. Also, the first four bands in the He I photoelectron (PE) spectrum of Cl_2O have been simulated by employing the iterative Franck–Condon analysis (IFCA) method.¹³ The IFCA treatment makes use of ab initio force constants for both the neutral and a cationic state, and the experimental geometry⁶ of the neutral molecule. The geometric parameters were obtained for the cationic states through a systematic variation of the cationic geometries, until the simulated spectra best matched the observed He I PE spectra.⁵ For two of the PE bands, the simulations, including the consideration of “hot” bands, have confirmed the assignments of the observed vibrational structure in the experimental

[†] Department of Applied Biology and Chemical Technology, Hong Kong Polytechnic University

[‡] Department of Chemistry, University of Southampton.

spectrum.⁵ In the case of the second band, the vibrational assignment has been revised.

2. Theoretical Considerations and Computational Details

The main aim of the ab initio calculations in this work was to obtain reliable minimum-energy geometries and harmonic vibrational frequencies for the neutral electronic ground state of Cl_2O and its low-lying cationic states, so as to carry out subsequent Franck–Condon factor (FCF) calculations and simulations of PE bands. The (U)MP2/6-311G(2d) level of calculation was first employed. Geometry optimization and vibrational frequency calculations on the ground states of the neutral and cation were completed. However, the MP2 level was found to be inadequate for the \tilde{X}^2B_1 cationic state, giving one imaginary frequency (for the b_2 asymmetric stretch). The QCISD/6-31G* (UQCISD/6-31G* for the cationic states) level of calculation was then employed and was found to be satisfactory for the neutral ground state and the four cationic states (see Results and Discussion), with the exception of the harmonic vibrational frequency calculation of the \tilde{C}^2A_2 state of the Cl_2O^+ . For the frequency calculation on the \tilde{C}^2A_2 cationic state at the QCISD level, there were excessive iterations in the QCISD energy evaluation at some point of the numerical second derivative calculations. Consequently, it was not possible to obtain the harmonic frequencies at the QCISD level for this state. To obtain the harmonic vibrational frequencies for the \tilde{C}^2A_2 state, CASSCF(7,6,nroot=2)/6-311+G(2d) and CASSCF(7,8,nroot=2)/6-311+G(2d) geometry optimization and frequency calculations were carried out only for this state. Additionally, the AIEs and VIEs for the four lowest PE bands were computed using the RCCSD(T)/aug-cc-pVQZ method with the QCISD/6-31G* optimized geometry.

All of the QCISD and CASSCF calculations were carried out using GAUSSIAN 98¹⁴ and all of the RCCSD(T) calculations were carried out using MOLPRO98,¹⁵ on the DEC8400 cluster at the Rutherford–Appleton Laboratory (EPSRC, UK) and SGI workstations at the Hong Kong Polytechnic University.

The principles involved in the FCF calculations and spectral simulations have been described previously.^{13,16} Briefly, the method is based on the harmonic oscillator model and includes the Duschinsky effect.¹⁷ In the IFCA procedure, the ground state neutral geometric parameters are held at the experimentally determined values,^{6,7} and the initial ionic geometry is obtained from the computed geometry change on ionization. The ionic geometric parameters are then varied slightly to give good agreement with the experimental vibrational band envelope. The ab initio force constant matrix (or F matrix) in the ionic state is assumed to be unchanged as the geometry (or G matrix) is changed slightly. Consequently, according to the Wilson GF formalism,¹⁸ the vibrational frequencies will change as the geometry is changed, but it was found that the differences between the refined and the ab initio values were less than 15 cm^{-1} in all cases of this work. The experimental structural parameters of the neutral molecule available in the literature⁶ were utilized in the IFCA computational procedure with no modification. Each vibrational component in a simulated photoelectron band was represented by a Gaussian function (with a fwhm of 20 meV, as estimated from the experimental spectra), with relative intensity of vibrational components given by the computed Franck–Condon factors. Hot bands were included by assuming a Boltzmann distribution in the initial state. The good agreement between the simulated and the observed first band suggests that the assumption of a Boltzmann distribution is a valid one. It was found that for the first PE band, where

TABLE 1: Calculated Geometries (Bond Length in Å/Bond Angle in Degrees) for the Neutral and the Four Lowest Lying Cationic States of Cl_2O

states	experimental values ^a		ab initio values	IFCA values
\tilde{X}^1A_1	1.695	87/110.886	1.730/111.31 ^b	
\tilde{X}^2B_1			1.672/117.82 ^b	1.640 ± 0.004/117.3 ± 0.3
\tilde{A}^2B_2			1.726/94.84 ^b	1.705 ± 0.007/100.1 ± 0.4
\tilde{B}^2A_1			1.671/132.41 ^b	1.637/131.99 ^e
\tilde{C}^2A_2			1.782/104.22 ^c	1.725 ± 0.004/108.9 ± 0.5
			1.805/105.43 ^d	
			1.739/108.87 ^b	

^a Refs 6 and 7. ^b At the QCISD/6-31G* level. ^c At the CASSCF(7,8,nroot=2)/6-311+G(2d) level. ^d At the CASSCF(7,6,nroot=2)/6-311+G(2d) level. ^e These values are obtained by combining the experimental bond length and bond angle of the \tilde{X}^1A_1 state (column 2) with the computed geometric changes upon ionization to the \tilde{A}^2B_2 state at the QCISD/6-31G* level (column 3).

TABLE 2: Vibrational Frequencies ($\nu_1/\nu_2/\nu_3$ in cm^{-1})^a for the Neutral and the Four Lowest Energy Cationic States of Cl_2O

states	experimental values ^b	ab initio values	IFCA values
\tilde{X}^1A_1	642/296/686	653.8/299.6/717.4 ^c	657.3/303.9/716.0 ^f
\tilde{X}^2B_1	678/347/-	681.7/320.3/648.3 ^c	686.0/324.5/646.8 ^g
\tilde{A}^2B_2	- /290/-	749.9/278.8/652.1 ^c	726.0/291.4/671.1 ^g
\tilde{B}^2A_1	- /282/-	561.8/283.6/579.7 ^c	564.3/288.2/578.9 ^g
\tilde{C}^2A_2	613/307/-	569.5/262.1/411.6 ^d	559.0/275.8/421.0 ^g
		565.1/259.0/483.6 ^e	

^a The two a_1 modes of ν_1 and ν_2 correspond to symmetric stretching and angle bending motions, whereas the b_1 mode of ν_3 corresponds to the asymmetric stretching motion (see text also). ^b Ref 5. ^c At the QCISD/6-31G* level. ^d At the CASSCF(7,8,nroot=2)/6-311+G(2d) level. ^e At the CASSCF(7,6,nroot=2)/6-311+G(2d) level. ^f These frequencies correspond to the IFCA values at the experimental geometry.^{5,6} (see text). ^g These frequencies correspond to the values at the IFCA geometries as given in Table 1.

TABLE 3: Calculated Adiabatic and Vertical Ionization Energies (AIE/VIE in eV) of the Four Lowest Energy Cationic States

states	AIE/VIE		
	experimental values ^a	ab initio values ^b	IFCA value
\tilde{X}^2B_1	10.887/10.971	11.007/11.199	
\tilde{A}^2B_2	12.016/12.297	11.983/12.371	12.159/12.304 ^c
\tilde{B}^2A_1	≤12.453/12.593	12.454/12.898	12.271/12.593 ^d
\tilde{C}^2A_2	12.742/12.742	12.842/12.851	

^a Ref 5. ^b At the RCCSD(T)/aug-cc-pVQZ//QCISD/6-31G* level of calculation. ^c The AIE value is the observed position of the fifth vibrational peak in the second band of the He I PE spectrum from ref 5; see text. ^d The VIE position was set to the observed VIE position from ref 5; see text.

the hot bands were most clear, a temperature of 300 K gave the best match between the simulated and observed hot bands. Therefore, for the three higher IE bands, a vibrational temperature of 300 K was also used. The experimental AIEs (see Table 3) were used, except otherwise stated, in the simulation of each PE band.

3. Results and Discussion

3.1 Ab Initio Calculations: Optimized Geometry and Vibrational Frequencies. The results obtained from the ab initio calculations carried out on the neutral ground state and the four lowest lying cationic states of Cl_2O are summarized in Tables 1–3. For the \tilde{X}^1A_1 state, the experimental values for the equilibrium geometric parameters and vibrational frequencies are available for comparison. The agreement between the

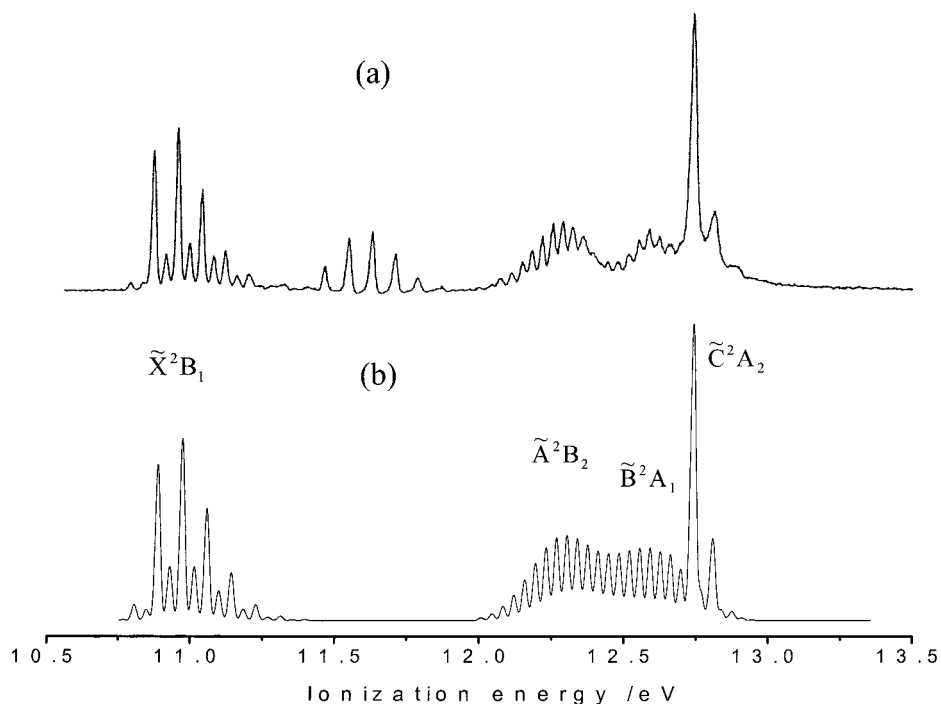


Figure 1. Full He I PE spectra of Cl_2O : (a) observed and (b) simulated (see text for details). The vibrational progression in the 11.4 to 11.8 eV region of the observed spectrum is due to Cl_2 (see ref 5).

theoretical and experimental geometric parameters can be considered as satisfactory, particularly for the bond angle. Good agreement between the computed and observed vibrational frequencies provides confidence that the ab initio force constants obtained at the QCISD/6-31G* level of calculation should be reasonably reliable and adequate for the subsequent FCF calculations.

For the cationic states, there are no available experimentally derived geometric parameters prior to this work. For the vibrational frequencies, some experimental values are available from the PE spectra (see Table 2). For the \tilde{X}^2B_1 , \tilde{A}^2B_2 , and \tilde{B}^2A_1 states, the agreement between the computed and the observed values is very good. It seems clear that the QCISD/6-31G* force constants are adequate, at least for the subsequent FCF calculations. For the \tilde{C}^2A_2 state, for which only CASSCF frequencies were obtained here, the agreement is not as good, but can be considered as reasonable. The two CASSCF calculations with different active spaces gave significantly different minimum-energy geometries, but similar vibrational frequencies. As the active space used in the CASSCF method increases, the optimized geometric parameters obtained appear to converge to the QCISD values (Table 1). Thus, the CASSCF(7,8,root=2)/6-311+G(2d) bond length (1.7821 Å) is closer to its QCISD value (1.7391 Å) than it is to the CASSCF(7,6,root=2)/6-311+G(2d) value of 1.8045 Å. The CASSCF(7,8,root=2)/6-311+G(2d) bending frequency of 262 cm^{-1} is slightly better than the CASSCF(7,6,root=2)/6-311+G(2d) value of 259 cm^{-1} (Table 2), when compared with the observed vibrational spacing of 307 cm^{-1} .¹ The CASSCF bond angles of 104.2° and 105.4° are probably too small because, with the rather large computed change in the bond angle at the CASSCF level upon ionization to this cationic state, a longer vibrational progression in the bending mode ν_2' in the simulated spectrum than that which was observed would be expected. It is clear that the QCISD bond angle of 108.9° for the \tilde{C}^2A_2 state is closer to the neutral QCISD angle of 111.3° than the CASSCF bond angles. The observed vibrational structure of the fourth band shows one major vibrational series, assigned to the symmetric

stretching mode, with only a weak shoulder assigned to the bending mode.⁵ Thus, it seems that the computed QCISD geometry change upon ionization for the fourth band, especially for the bond angle, is more consistent with the experimental observations than that of the CASSCF counterparts. In view of these considerations, for the \tilde{C}^2A_2 state, the CASSCF(7,8) force constants were used in the IFCA procedure, but the QCISD geometry was used as the initial geometry for the upper cationic state.

3.2 Adiabatic and Vertical Ionization Energies of the PE Bands. The AIEs/VIEs were calculated at the RCCSD(T)/aug-cc-pVQZ//QCISD/6-31G* level for the four PE bands of Cl_2O and are compared with the experimental AIEs and VIEs in Table 3. It can be seen that, in general, all of the computed AIEs and VIEs agree very well with the experimental values. Thus, the assignments of the cationic states to the PE bands can be confirmed unambiguously by the present ab initio calculations.

Examining the results in detail, the calculated AIEs and VIEs are slightly larger than the corresponding observed values for ionization to the cationic \tilde{X}^2B_1 , \tilde{B}^2A_1 , and \tilde{C}^2A_2 states. For ionization to the cationic \tilde{A}^2B_2 state, the computed AIE and VIE are slightly lower and higher than those of the respective corresponding measured values. Nevertheless, for all four PE bands, the differences between the computed and observed AIEs and VIEs are within 0.12 and 0.305 eV, respectively. In addition, the calculated AIE–VIE separations for each band agree to within 0.1 eV with the experimental values, with the exception of the third band, for which the observed AIE value reported in ref 5 is an estimate ($\leq 12.453\text{ eV}$) due to overlap by the second band. The computed AIE–VIE separation for the third band suggests that the actual AIE position is lower than the experimentally estimated one by over 0.3 eV.

3.3 Simulation of Vibrational Structures of the PE Bands of Cl_2O . Figure 1 shows the simulated (after application of the IFCA procedure for each band) and observed PE spectra of Cl_2O in the region of 10.6 to 13.2 eV. The relative band intensities have been chosen to match those in the experimental spectrum. It can be seen that the overall agreement is very good. The

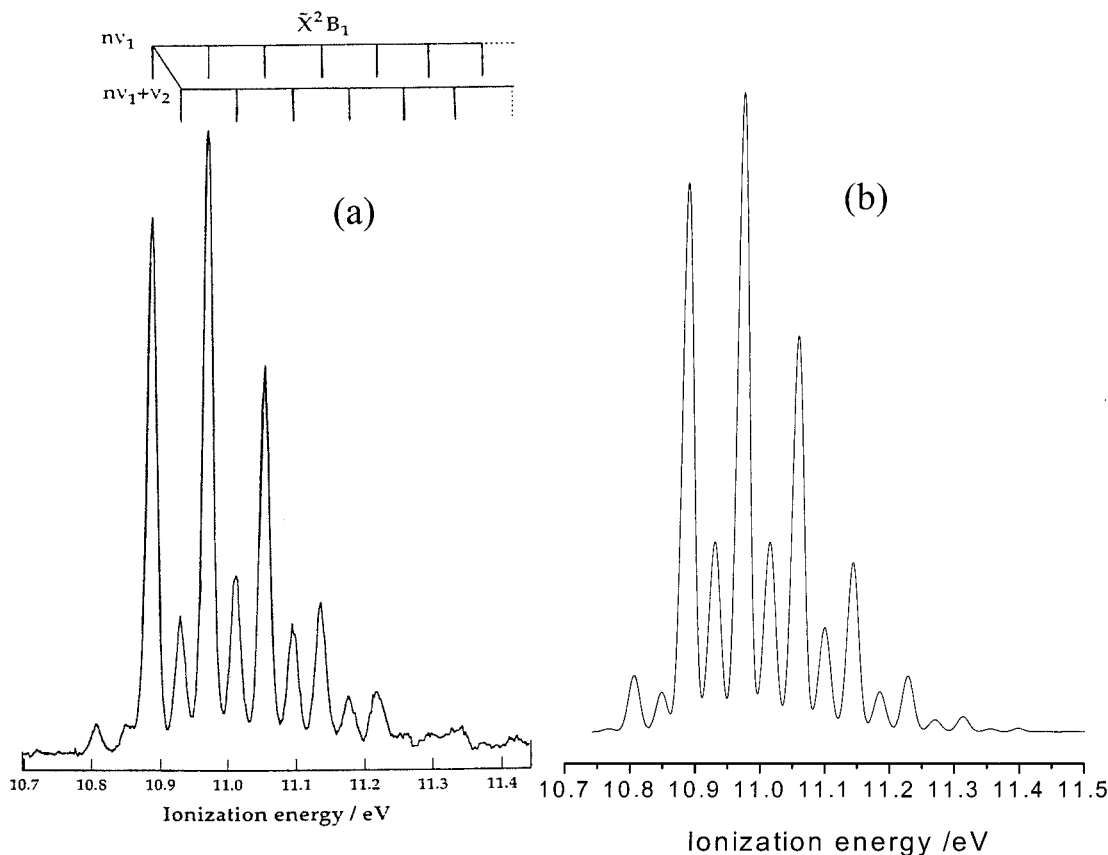


Figure 2. Expanded first band of the He I PE spectrum: (a) experimental spectrum from ref 5 and (b) simulated spectrum, employing the IFCA geometry of the \tilde{X}^2B_1 state (see text and Table 1).

simulated spectrum, which matches best with the experimental spectrum,⁵ has the IFCA geometries of the cationic states given in Table 1. The expanded first and fourth simulated PE bands and the corresponding experimental bands are compared in more detail in Figures 2 and 3. Because the second and third bands overlap extensively, it was not possible to study them separately, and their expanded simulated spectra are shown together in Figure 4.

For the third band, the AIE position cannot be identified from the experimental spectrum. Consequently, the IFCA simulation procedure was not carried out for this band. The ab initio geometry change upon ionization was employed together with the experimental geometry of the neutral molecule to produce the simulated spectrum (see footnote *e* of Table 1). The vibrational component, which was calculated to have the strongest overall relative FCF, was set to match the observed strongest peak (the observed VIE position). Then the IFCA procedure was carried out for the second band, including the contribution from the simulated spectrum of third band obtained as described above. More details of the comparison between the simulated and observed spectra are given below.

The IFCA procedure could be used for the first and fourth bands, and the agreement between the simulated and observed spectra of these bands, as shown in Figures 2 and 3, is good (see Concluding Remarks). The comparison between the simulated and observed spectra of the first band (Figure 2) in the low IE region, which included the effects of hot bands, enabled a vibrational temperature of 300 K to be reliably established, as mentioned above. For cases in which this temperature was used in the simulations of the other bands, it was found that the contributions of hot bands to the second and third bands were quite strong (from population of the excited vibrational levels of the bending mode in the neutral molecule;

see Figures 5 and 6). To show the various contributions of the different vibrational series, the computed FCFs of the vibrational progressions with reasonably strong intensities are displayed in bar diagrams for the second and third bands, respectively, in Figures 5 and 6. It can be seen that the FCF intensity patterns for the hot band series between these two PE bands are very different. In particular, for the second PE band (Figure 5), the low IE components of the hot band series are quite strong and are of comparable intensities to those in the high IE region. Consequently, the observed low IE components of the second band must be due to hot bands, rather than the main $(0, v_2', 0) \leftarrow (0, 0, 0)$ series, as was assigned in ref 5. On the basis of FCF calculations and simulations carried out in this work, the first four observable components of the second band are almost certainly due to hot bands. In this connection, the AIE position of the second band would be at the fifth observed vibrational component, with a measured value of 12.159 eV, which was assigned to the $v_2' = 4$ of the main series in ref 5. In addition, on the basis of our spectral simulations, the observed VIE position at 12.297 eV is now due to the $(0, 4, 0) \leftarrow (0, 0, 0)$ ionization. It should be noted that for this feature, there are significant contributions from other vibrational series (see Figure 5), including those of the overlapping third band. For the main vibrational series $(0, v_2', 0) \leftarrow (0, 0, 0)$, the $v_2' = 3$ component is the strongest within the series. However, contributions from "hot" bands and other series, as mentioned above, have changed the VIE position to the $v_2' = 4$ component.

For the third PE band, the contribution of "hot" bands seems to be slightly less strong, as compared with that to the second band (see Figures 5 and 6), and the pattern of the vibrational structure of the hot bands is quite different, as mentioned above. An attempt has been made to obtain the best simulation of the third band by matching the strongest component in the simula-

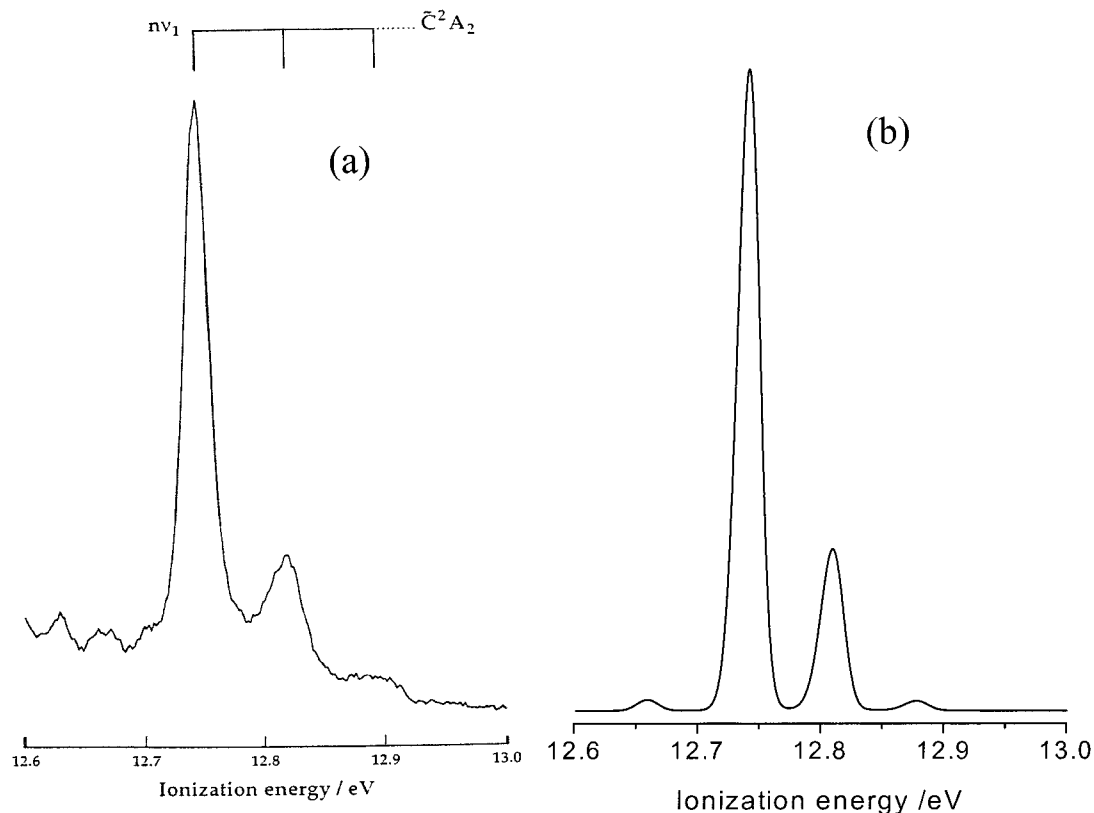


Figure 3. Expanded fourth band of the He I PE spectrum: (a) experimental spectrum from ref 5; (b) simulated spectrum, employing the IFCA geometry of the \tilde{C}^2A_2 state (see text and Table 1). Note that the first weak peak in the simulated spectrum (b) at ca. 12.65 eV is a hot band, arising from the $v_1'' = 1$ level of the neutral molecule.

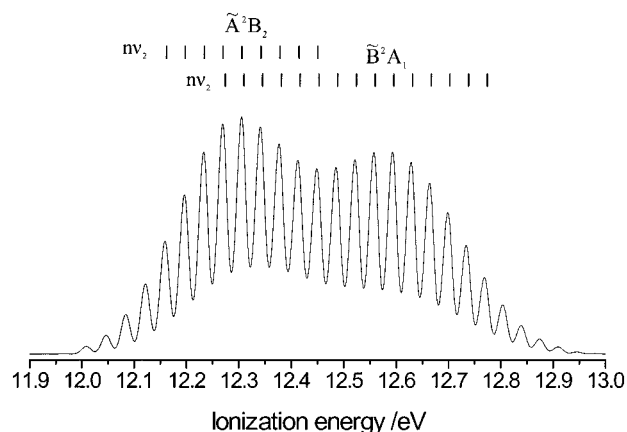


Figure 4. Expanded second and third bands of the He I PE spectrum: simulated spectrum, employing the IFCA geometry of the \tilde{A}^2B_2 state (see Table 1 and text for details).

tion with the observed VIE position, as the AIE position is not clear from the observed spectrum. In these simulations, contributions from the second and fourth bands were included. This is the best that can be done in view of the severe overlapping band problem that occurs with the third band. Because the IFCA procedure could not be carried out for this band, the main drawback in this simulation is the use of the ab initio geometry change upon ionization, which is assumed to be close to the true one. On the basis of the FCF calculations and simulations, the measured VIE position, 12.593 eV, of the third band can be assigned to the $(0,9,0) \leftarrow (0,0,0)$ ionization, and the AIE position would then have a value of 12.271 eV, which is significantly lower than the experimentally estimated value (Table 3). Thus, the revised experimental AIE–VIE separation

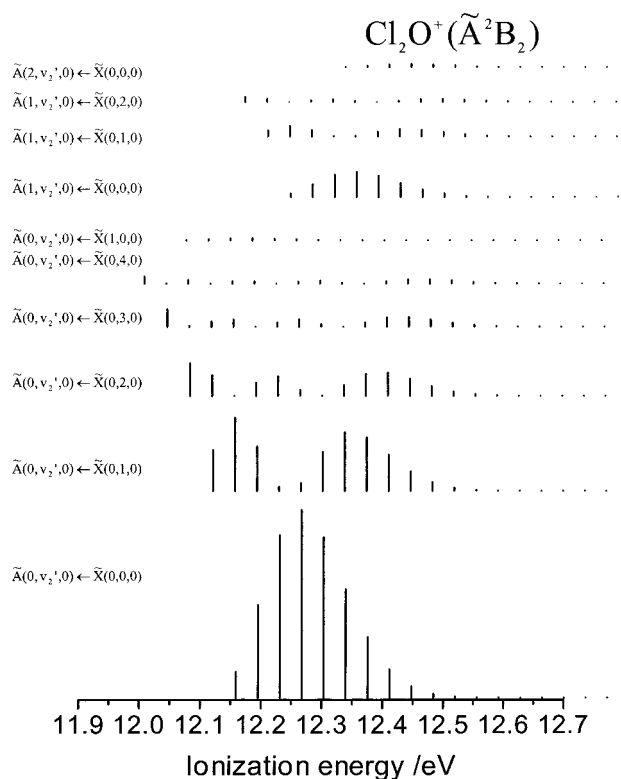


Figure 5. Computed FCFs of the vibrational series with relatively stronger intensities for the $\tilde{A}^2B_2 \leftarrow \tilde{X}^1A_1$ ionization, including hot bands, at a temperature of 300 K, assuming Boltzmann distributions

of 0.322 eV compares well with the RCCSD(T)/aug-cc-pVQZ//QCISD/6-31G* value of 0.444 eV.

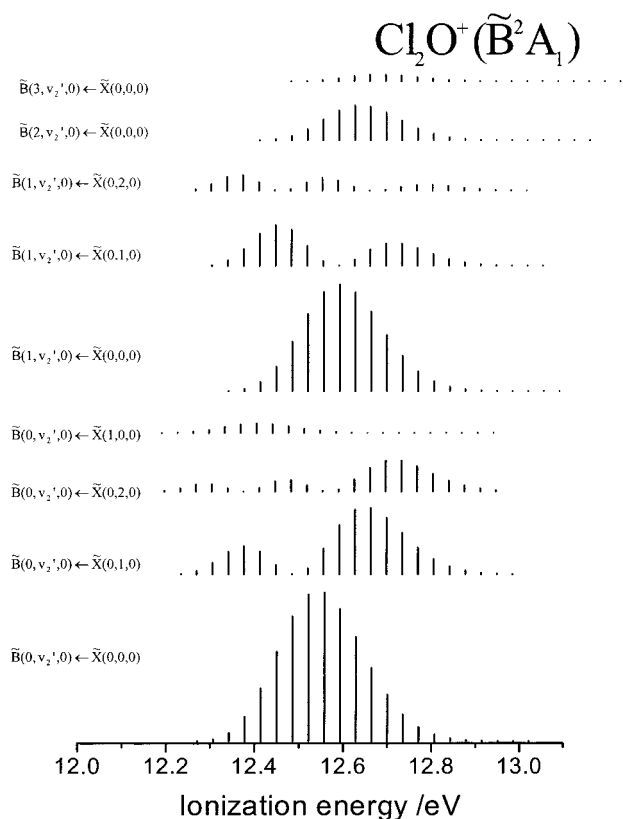


Figure 6. The computed FCFs of the vibrational series with relatively stronger intensities for the $\tilde{B}^2A_1 \leftarrow \tilde{X}^1A_1$ ionization, including hot bands, at a temperature of 300 K, assuming Boltzmann distributions.

4. Concluding Remarks

In this investigation, high-level ab initio calculations on the neutral ground state and the four lowest lying cationic states of Cl_2O are reported. The assignments of the cationic states made in an earlier study of the He I PE spectra⁵ have been confirmed. FCF calculations and spectral simulations, which include allowance for hot bands, have led to revised assignments of the vibrational structure observed in the second PE band, the $\tilde{A}^2B_2 \leftarrow \tilde{X}^1A_1$ ionization. As a result of this revision, the AIE position for this band is also revised. The error in the new AIE position depends on the reliability of the revised vibrational assignments, which is probably within one quantum in the bending mode. In this connection, the uncertainty associated with the revised AIE value (12.159 eV) can be estimated to be on the order of ± 0.037 eV (≈ 300 cm^{-1}), which is the observed vibrational spacing of the bending mode of the upper state. In summary, the usefulness of FCF calculations and spectral simulations is clearly demonstrated in the study of the second PE band of Cl_2O .

For the third PE band of the $\tilde{B}^2A_1 \leftarrow \tilde{X}^1A_1$ ionization, despite being heavily overlapped by the second and fourth band, a major effort was made to simulate its PE spectrum. As a result, a more reliable AIE position than that of the estimate from the previous experimental study⁵ has been obtained. Although the uncertainty associated with this AIE value of 12.271 eV will be larger than that obtained above for the second band, for the $\tilde{A}^2B_2 \leftarrow \tilde{X}^1A_1$ ionization, the AIE–VIE separation obtained with this revised AIE value agrees with the RCCSD(T) AIE–VIE separation to within 0.122 eV. In this connection, an estimated uncertainty of 0.15 eV for the third AIE value seems reasonable. Although this uncertainty is rather large, it is at least possible, using the

present FCF calculations and spectral simulations, to obtain a more reliable AIE position than that which was available previously.

IFCA procedures were carried out for the first, second, and third band of the He I PE spectrum of Cl_2O . With the experimental geometry of the neutral ground state, geometrical parameters of the \tilde{X}^2B_1 , \tilde{A}^2B_2 , and \tilde{C}^2A_2 states of Cl_2O^+ have been derived experimentally for the first time. For the first band, the overall agreement between the simulated and the observed spectra is very good, with the exception of the $(0,1,0) \leftarrow (0,0,0)$ peak, which has its simulated relative intensity slightly higher than the observed one (Figure 2). In the IFCA procedure, attempts were made to improve the agreement for this peak. It was found that the IFCA r_e value was critical in affecting the relative intensity of this peak, and achieving a better agreement for this peak had led to a poorer agreement for the main ν_1 series. Because it seems reasonable to place more weight on the stronger main stretching series than the weaker bending progression in the comparison between the simulated and observed spectra, the simulation as shown in Figure 2 has been concluded to be the best match. With this simulation, the IFCA r_e value is 1.640 Å for the \tilde{X}^2B_1 cationic state (Table 1). A rather large uncertainty of ± 0.004 Å has been given for this IFCA r_e value (Table 1), including allowance for the slight discrepancy between the simulated and observed spectra. For the \tilde{A}^2B_2 and \tilde{C}^2A_2 states, the uncertainties of the geometrical parameters obtained here are also large (Table 1). This is partly because of overlapping band problems and partly because only a vibrational series of one of the two symmetric modes is excited extensively in each case (the bending mode in the \tilde{A}^2B_2 state and the stretching mode in the \tilde{C}^2A_2 state). The lack of well-resolved vibrational structure in the other symmetric mode has hampered the extraction of information from the observed spectra. For the \tilde{A}^2B_2 state, the uncertainty in the revised vibrational assignments has been included in the estimation of the uncertainty associated with the IFCA bond angle. Nevertheless, the information derived in this study, notably the vibrational assignments, new AIEs, ionic state geometries, and frequencies for the four lowest states of Cl_2O^+ represent a considerable body of new information.

Acknowledgment. The authors are grateful to the Research Grant Council (RGC) of the Hong Kong Special Administration Region (HKSAR), the Research Committee of the Hong Kong Polytechnic University, and the Leverhulme Trust for financial support. The EPSRC UK is acknowledged for the computational resources made available to them via the Computational Facility for Computational Chemistry in UK.

References and Notes

- (1) Rowland, F. S. *Annu. Rev. Phys. Chem.* **1991**, *42*, 731.
- (2) Sander, S. P.; Friedl, R. R.; Francisco, J. S. In *Progress and Problems in Atmospheric Chemistry*; Barker, J. R., Ed.; World Scientific: Singapore, 1995.
- (3) Cornford, A. B.; Frost, D. C.; Herring, F. G.; McDowell, C. A. *J. Chem. Phys.* **1971**, *55*, 2820.
- (4) Thorn, R. P., Jr.; Stief, L. J.; Kuo, S.-C.; Klemm, R. B. *J. Phys. Chem.* **1996**, *100*, 14 178.
- (5) Motte-Tollet, F.; Delwiche, J.; Heinesch, J.; Hubin-Franskin, M.-J.; Gingell, J. M.; Jones, N. C.; Mason, N. J.; Marston, G. *Chem. Phys. Lett.* **1998**, *284*, 452.
- (6) Herberich, G. E.; Jackson, R. H.; Millen, D. J. *J. Chem. Soc. A* **1966**, 336.
- (7) Nakata, M.; Sugic, M.; Takeo, H.; Matsumura, C.; Fukuyama, T.; Kuchitsu, K. *J. Mol. Spectrosc.* **1981**, *86*, 241.
- (8) Dunitz, J. D.; Jedberg, K. *J. Chem. Soc.* **1950**, 72, 3108.
- (9) Bru, L.; Rodriguez, P.; Cubero, M. *J. Chem. Phys.* **1952**, *20*, 1069.

- (10) Nelson, C. M.; Moore, T. A.; Okumura M.; Minton, T. K. *J. Chem. Phys.* **1994**, *100*, 8055.
- (11) Nickolaisen, S. L.; Miller, C. E.; Sander, S. P.; Hand, M. R.; Williams, I. H.; Francisco J. S. *J. Chem. Phys.* **1996**, *104*, 2857.
- (12) Luke, B. T. *THEOCHEM* **1995**, *332*, 283.
- (13) Chau, F. T.; Dyke, J. M.; Lee, E. P. F.; Wang, D. C. *J. Electron. Spectrosc. Relat. Phenom.* **1998**, *97*, 33.
- (14) *Gaussian 98* (Revision A.6), Frisch, M. J.; Trucks, G. W.; Schlegel, H. B.; Scuseria, G. E.; Robb, M. A.; Cheeseman, J. R.; Zakrzewski, V. G.; Montgomery, J. A.; Stratmann, R. E.; Burant, J. C.; Dapprich, S.; Millam, J. M.; Daniels, A. D.; Kudin, K. N.; Strain, M. C.; Farkas, O.; Tomasi, J.; Barone, V.; Cossi, M.; Cammi, R.; Mennucci, B.; Pomelli, C.; Adamo, C.; Clifford, S.; Ochterski, J.; Petersson, G. A.; Ayala, P. Y.; Cui, Q.; Morokuma, K.; Malick, D. K.; Rabuck, A. D.; Raghavachari, K.; Foresman, J. B.; Cioslowski, J.; Ortiz, J. V.; Stefanov, B. B.; Liu, G.; Liashenko, A.; Piskorz, P.; Komaromi, I.; Gomperts, R.; Martin, R. L.; Fox, D. J.; Keith, T.; Al-Laham, M. A.; Peng, C. Y.; Nanayakkara, A.; Gonzalez, C.; Challacombe, M.; Gill, P. M. W.; Johnson, B. G.; Chen, W.; Wong, M. W.; Andres, J. L.; Head-Gordon, M.; Replogle E. S.; Pople, J. A.; Gaussian, Inc., Pittsburgh, PA, 1998.
- (15) *MOLPRO* version 98.1 is a package of ab Initio programs written by Werner, H.-J. and Knowles, P. J., with contributions from Amos, R. D.; Berning, A.; Cooper, D. L.; Deegan, M. J. O. A.; Dobbyn, J.; Eckert, F.; Hampel, C.; Leininger, T.; Lindh, R.; Lloyd, A. W.; Meyer, W.; Mura, M. E.; Nicklass, A.; Palmieri, P.; Peterson, K.; Pitzer, R.; Pulay, P.; Rauhut, G.; Schütz, M.; Stoll, H.; Stone A. J.; Thorsteinsson, T.; 1998, University of Birmingham, UK.
- (16) Chen, P. In *Unimolecular and Bimolecular Ion molecule Reaction Dynamics*; Ng, C. Y., Baer, T., Powis, I., Eds.; Wiley: Chichester 1994.
- (17) Duschinsky, F. *Acta Physiochim. URSS* **1937**, *7*, 551.
- (18) Wilson, E. B., Jr.; Decius, J. C.; Cross P. C. *Molecular Vibrations*; McGraw-Hill: New York, 1955.